which has been published in **Acs chemical neuroscience** 2019, vol 10 (6), 2848-2857.
https://doi.org/10.1021/acschemneuro.9b00083

Pyrazine-fused triterpenoids block the TRPA1 ion channel *in vitro* and inhibit TRPA1-mediated acute inflammation *in vivo*

Ilari Mäki-Opas[†], Mari Hämäläinen[†], Lauri J. Moilanen[†], Raisa Haavikko[‡], Tiina J. Ahonen[‡], Sami Alakurtti[‡,§], Vânia M. Moreira[‡,"], Katsuhiko Muraki[⊥], Jari Yli-Kauhaluoma[‡] and Eeva Moilanen[†]

[†]The Immunopharmacology Research Group, Faculty of Medicine and Health Technology, Tampere University and Tampere University Hospital, Tampere, Finland

[‡]Drug Research Program, Division of Pharmaceutical Chemistry and Technology, Faculty of Pharmacy, University of Helsinki, Helsinki, Finland

[§]VTT Technical Research Centre of Finland Ltd, Espoo, Finland

"Strathclyde Institute of Pharmacy and Biomedical Sciences, University of Strathclyde, Glasgow, UK

[⊥]Laboratory of Cellular Pharmacology, School of Pharmacy, Aichi Gakuin University, Nagoya, Japan

ABSTRACT

TRPA1 is a non-selective cation channel, most famously expressed in non-myelinated nociceptors. In addition to being an important chemical and mechanical pain sensor, TRPA1 has more recently appeared to have a role in inflammation as well. Triterpenoids are natural products with anti-inflammatory and anti-cancer effects in experimental models. In this paper, thirteen novel triterpenoids were created by synthetically modifying betulin, an abundant triterpenoid of the genus *Betula* L. and their TRPA1-modulating features were examined. Fluo 3-AM protocol was used in the initial screening, in which six out of the fourteen tested triterpenoids inhibited TRPA1 in a statistically significant manner. In subsequent whole-cell patch clamp recordings, the two most effective compounds (pyrazine-fused triterpenoids **8** and **9**) displayed a reversible and dose and voltage-dependent effect to block the TRPA1 ion channel at submicromolar concentrations. Interestingly, the TRPA1-blocking action was also evident *in vivo*, as compounds **8** and **9** both alleviated TRPA1-agonist induced acute paw inflammation in mice. The results introduce betulin-derived pyrazine-fused triterpenoids as promising novel antagonists of TRPA1 that are potentially useful in treating diseases with a TRPA1-mediated adverse component.

KEYWORDS: Transient receptor potential channels, TRPA1, inflammation, pain, natural compounds, triterpenoids

INTRODUCTION

Transient receptor potential ankyrin 1 (TRPA1) is a cation channel expressed predominantly in Aδ- and C-type nociceptive nerve fibers mediating chemical and mechanical pain. TRPA1 is a physiological chemoreceptor for potentially harmful exogenous chemicals and its activation causes immediately perceivable and often painful sensations.[1,2] Indeed, there are many naturally occurring irritants that activate TRPA1 e.g. allicin in garlic (*Allium sativum* L.), cinnamaldehyde in cinnamon (*Cinnamomum* Schaeff.) and allyl isothiocyanate (AITC) in mustard oil.[3-5]

There is increasing data supporting the idea that TRPA1 ion channel also plays a critical role in inflammation.[1] Pharmacological blockade and genetic deletion of TRPA1 have been shown to alleviate nociception and inflammation in animal models such as carrageenan-induced paw inflammation,[6] monosodium iodoacetate-induced arthritis,[7] monosodium urate crystals-induced gouty arthritis and formalin-induced pain.[8-10] These adverse effects of TRPA1 activation were not due to a direct effect of the disease-inducing exogenous substance on the ion channel but attributable to endogenous activation of TRPA1. Indeed, endogenous compounds capable of opening the TRPA1 channel have recently been characterized and they include factors released in inflammatory conditions such as reactive oxygen and nitrogen species (ROS and RNS), bradykinin and some prostaglandins.[5,11] The emerging dualistic role of TRPA1 in nociception and inflammation has revealed TRPA1 as a promising drug target. It has been speculated that blockade of TRPA1 is likely to provide direct alleviation of pain and additionally attenuate inflammation. However, although there is a wide spectrum of compounds known to activate TRPA1, only a few blockers have been identified.

Betulin (**1**) is a widely studied triterpenoid, which can be found in the birch tree bark (*Betula* sp. L.). Other triterpenoids are present in olives and apple peel and are thought to contribute to some of the health promoting effects of these foodstuffs: Betulin (**1**) and some related triterpenoids have

been found to possess anti-inflammatory properties.[12-15] There is also evidence of their therapeutic potential against cancer, HIV and protozoal diseases.[16-25]

Based on our preliminary screening results, we postulated that some of the pharmacological features of triterpenoids might be attributable to blockade of TRPA1. In the present study, we utilized two *in vitro* protocols: the Fluo 3-AM intracellular Ca^{2+} measurement and whole-cell patch clamp current recording, as well as an *in vivo* model of acute TRPA1-mediated inflammation to study the effects of betulin (**1**) and a series of its derivatives (**2 – 14**) on TRPA1.

RESULTS

Chemistry. Thirteen triterpenoids **2-14** were synthesized as described previously and their structures are shown in Figure 1, along with betulin (**1**).[20-22] In addition, a novel method to convert betulin to betulonic and further to betulinic acid was developed (Figure 2): First, betulin (**1**) was oxidized to betulonic aldehyde with air using palladium(II) acetate as a catalyst. The resulting betulonic aldehyde was further oxidized to betulonic acid (**2**) in one pot using sodium chlorite as an oxidant. Finally, the reduction of betulonic acid (**2**) with $NaBH_4$ produced betulinic acid (**3**) with a good yield.

Six of the fourteen triterpenoids inhibit TRPA1 *in vitro*. The antagonistic properties of the triterpenoids on TRPA1 were first screened at 10 µM concentrations using the Fluo 3-AM calcium measurement protocol in human TRPA1 (hTRPA1) transfected HEK293 cells. The cells were pre-incubated with the triterpenoids and thereafter TRPA1-mediated Ca^{2+}-influx was induced by adding the known TRPA1 activator AITC.

Six triterpenoids, namely compounds **5**, **6**, **7**, **8**, **9** and **14** inhibited AITC-induced Ca^{2+}influx at 10 µM concentration in a statistically significant manner. The results of the TRPA1-blocking activity of all triterpenoids studied are summarized in Table 1. The cytotoxicity of the compounds in the experimental conditions used was ruled out with the XTT assay.

The two most promising compounds **8** and **9** (Figure 3) were examined further in a broader range of concentrations up to 100 µM and a dose-dependent inhibition was observed with both compounds (Figure 4). The IC_{50} values of compounds **8** and **9** in the Fluo 3-AM Ca^{2+}-influx measurements were 9.5 and 7.5 µM, respectively.

Further experiments demonstrated that the triterpenoids **8** and **9** blocked AITC-induced Ca^{2+}-influx also in HEK293 cells transfected with mTRPA1 (Figure 5). In addition, compounds **8** and **9** at

concentrations up to 100 μM did not induce any detectable Ca^{2+}-influx in HEK293 cells transfected with either human or mouse TRPA1, ruling out an agonistic effect.

In whole-cell patch clamp recordings, triterpenoids 8 and 9 display a strong and reversible TRPA1-blocking activity. To verify the TRPA1 blocking ability of compounds **8** and **9**, we utilized the whole-cell patch clamp recording technique. In HEK293 cells transfected with hTRPA1, the AITC (50 μM)-induced ion currents through TRPA1 were strongly attenuated at a holding potential of -50 mV when the cells were treated with either compound **8** or **9** (Figure 6A and 6C). Interestingly, both compounds exerted a voltage-dependent blockade of TRPA1 channel currents (Figure 6B and 6D). The IC_{50} values of compounds **8** and **9** against HC-030031 sensitive TRPA1 channel currents at -100 mV and -50 mV were each 0.3 μM, whereas at +50 mV they were 1.3 μM, and at +100 mV, they were 1.8 μM and 4.4 μM, respectively (Figure 6E and 6F).

In additional experiments, we examined the reversibility of the inhibitory effects of compounds **8** and **9** on TRPA1. Since high concentrations of AITC may desensitize TRPA1 during the recordings, we exploited 10 μM AITC to activate TRPA1 in these experiments. As shown in Figure 7A-H, both pyrazine-fused triterpenoids (compounds **8** and **9**) exhibited inhibitory effects on 10 μM AITC-induced currents at a holding potential of -50 mV comparable to those seen with the 50 μM AITC-induced currents (see also Figure 6E and 6F). This suggests that the concentration of the TRPA1 agonist had little or no influence on the inhibitory effect of compounds **8** and **9**. After the current amplitude had stabilized during the application of compounds **8** and **9**, they were removed from the bathing solution while maintaining 10 μM AITC. The recovery of AITC-induced TRPA1 activation was complete after the withdrawal of 0.3 and 3 μM concentrations of compounds **8** and **9**; while the recovery was partial, but still obvious, after 30 μM concentrations of compounds **8** and **9** (Figure 7C, 7F, 7G and 7H). This demonstrates that compounds **8** and **9** are reversible blockers of hTRPA1 at concentrations up to 3 μM, but at 30 μM concentration the blockade is partially irreversible.

Triterpenoids 8 and 9 attenuate TRPA1-mediated acute inflammation *in vivo*. As compounds **8** and **9** were highly promising TRPA1 blockers *in vitro*, we determined whether they could inhibit TRPA1-mediated inflammation *in vivo*. Hence, the effects of compound **8** and **9** on AITC-induced acute inflammation were investigated in the mouse paw edema model. The mice were injected intraplantarly with the TRPA1 agonist AITC and the increase in the volume of the paw caused by the inflammatory edema was measured in mice pre-treated with the compounds and compared with those receiving vehicle only. Systemically administered compounds **8** (10 mg/kg, i.p.) and **9** (10 mg/kg, i.p.) both attenuated the AITC-induced inflammatory edema with an effect similar to the known TRPA1 antagonist HC-030031 (300 mg/kg, i.g.), used as a positive control. The results are summarized in Figure 8.

DISCUSSION

The present results clearly indicate that the two pyrazine-fused triterpenoids, compounds **8** and **9** (Figure 3), effectively inhibit TRPA1 activation in a dose-dependent manner *in vitro* and significantly attenuate acute inflammation mediated by TRPA1 *in vivo*. The observed blockade of both human and mouse TRPA1 channel *in vitro* suggests that the compounds' inhibitory effects on TRPA1-mediated conditions in mice are likely to be generalized to humans as well. Furthermore, in the whole-cell patch clamp recordings, the blocking effect of the compounds was completely reversible up to the concentrations of 3 μM.

The *in vivo* experiments demonstrated that compounds **8** and **9** attenuated TRPA1-mediated inflammation induced by AITC, indicating that these two triterpenoids when administered systemically have appropriate pharmacokinetics to ease paw inflammation, most likely by inhibiting TRPA1 activation. It is noteworthy that the two triterpenoids were active at doses lower than the widely used TRPA1 antagonist HC-030031. Mice exhibited no adverse effects due to treatment with the triterpenoids during the short duration of the experiment.

The detailed molecular mechanism of action of pyrazine-fused triterpenoids (compounds **8** and **9**) on TRPA1 channel cannot be determined based on the results of the present study though both triterpenoids inhibited the channel currents in a voltage-dependent manner. Previous studies on TRPA1 blockers have revealed versatile binding sites and mechanisms of actions: a very effective TRPA1 antagonist A-967079 seems to attach to the TRPA1 channel pore vestibule where it interacts with the phenyl moiety of F944,[26] the site of HC-030031 action is the N855 residue of the channel and interaction with the C-terminus region exerts synergistic effects on the inhibition.[27] Since compounds **8** and **9** exerted voltage-dependent blockade against TRPA1, it is possible that these triterpenoids interact with certain amino acid residues in the channel which are located close

to the electrical fields within the plasma membrane. In addition, HC-030031 has been reported to be a rapidly acting and reversible blocker.[10] Menthol is a terpene related compound, which has been shown to have an effect on TRPA1. Its binding site in mouse TRPA1 has been reported to be transmembrane domain 5, which is essential for the channel's ability to sense menthol. Nine other pore residues were also identified to account for the species-specific alteration of menthol's action as either agonist or antagonist of TRPA1.[28]

In the present study, we showed that the effects of the compounds **8** and **9** were reversible at least up to the concentration of 3 μM, while their action was only partly reversible at 30 μM concentration. Moreover, the recovery after the removal was relatively slow even at 0.3 μM, suggesting that these triterpenoids bind tightly to the TRPA1 channel. Since both compounds **8** and **9,** but not the other triterpenoids investigated, have a pyrazine ring in their structure (Figure 1), this moiety appears to be critical for their blocking efficacy, reversibility and/or recovery rate after their removal. The conversion of the carboxylic acid in compound **8** to the respective amide in compound **9** did not seem to affect the TRPA1 blocking properties of the compound. Even though the pyridine derivative compound **10** did not exert a blockade similar to compounds **8** and **9**, the effects of other six-membered rings on the 2,3-position should be determined in the future. Further extensive studies will be required to clarify the detailed molecular mechanisms of TRPA1-blocking by pyrazine-fused triterpenoids.

The IC_{50} values of compounds **8** and **9**, around 0.3 μM each at -50 mV in whole-cell patch clamp recordings against 50 μM AITC, were lower than that of the most widely used TRPA1 blocker HC-030031 (~1 μM against 5 μM AITC-induced human TRPA1 currents).[10] However, the IC_{50} values calculated from intracellular Ca^{2+} influx measurements were higher: 9.5 and 7.5 μM for compounds **8** and **9**, respectively. Similarly, the IC_{50} value of HC-030031 was higher in the Ca^{2+} measurement assay (6.2 μM) than in the patch clamp experiments.[10] It is also notable that IC_{50} values of compounds **8** and **9** were increased at positive membrane potentials in whole-cell patch clamp

experiments. This depolarization-induced reduction in the blockade of TRPA1 by both compounds **8** and **9** may in part explain the difference in IC_{50} values between Fluo 3-AM and whole-cell patch clamp experiments. The activation of TRPA1 induces depolarization of TRPA1-expressing HEK 293 cells in the Fluo 3-AM experiments and thus may attenuate the blocking efficacy of compounds **8** and **9** against TRPA1. For comparison to the identified IC_{50} value of 0.3 µM for betulin -derived compounds **8** and **9**, the naturally occurred stilbenoids pinosylvin and resveratrol have been shown to block TRPA1 activity with IC_{50} of 16.7 µM and 12,9 µM, in whole-cell patch clamp recordings, respectively,[29] and gallic acid with IC_{50} of 11 µM.[30] Recently described synthetically modified quinazolinone-based purinone **27** and N-isopropylglycine sulfonamide-based Compound **20** have increased potency while the most widely used traditional TRPA1 blockers are less potent than the compounds **8** and **9** identified in the present study.[31,32]

Laavola *et al.* have recently assessed the anti-inflammatory properties of compounds **8** and **9**.[15] A significant decrease of inducible nitric oxide synthase (iNOS) expression was observed in J774 macrophages treated with both compounds, which is likely to result in impaired production of nitric oxide (NO) in inflammatory conditions. As NO is a known TRPA1 activator,[11] compounds **8** and **9** may down-regulate TRPA1-mediated responses in inflammatory conditions both directly by blocking the channel (as shown in the present study) and indirectly by reducing the synthesis of endogenous TRPA1 activators such as NO. Moreover, the antagonistic effects of compounds **8** and **9** on TRPA1 channels may at least partially explain the previously reported attenuating effects of these compounds on inflammatory gene expression,[15] because TRPA1 activation has been shown to up-regulate the expression of pro-inflammatory factors, like cyclo-oxygenase-2, and interleukins 1, 6, and 8 in inflammatory conditions.[6,7,33-35]

The present results have laid the foundation for a wider assessment of the effects of pyrazine-fused triterpenoids in different animal models of diseases involving TRPA1 activation. If one considers the positive effects of other TRPA1 blockers, treatment of neuropathic pain has travelled the longest

path; phase II clinical trials of the compound GRC 17536 have been conducted, with favorable results.[36] Some novel directions in TRPA1 research have emerged: TRPA1 has a notable role in the pathogenesis of allergic contact dermatitis and therefore TRPA1 blockers might be useful in its treatment.[37] Our recent studies have shown that in primary human articular chondrocytes TRPA1 is expressed and that TRPA1 blockers and/or genetic deletion of TRPA1 can alleviate pain and inflammation in experimental models of osteoarthritis and gout.[7,8,33] Other inflammatory conditions such as colitis and asthma are also potential targets of TRPA1 blockers.[38,39] The most widely used TRPA1 blocker in animal experiments, HC-030031, was unfortunately discovered to possess poor pharmacokinetic properties.[40] Therefore, the pharmacokinetic profile as well as the safety profile of compounds **8** and **9** should be characterized in the future, although our preliminary data did not reveal any obvious concerns.

In conclusion, this study discovered two pyrazine-fused triterpenoids (compounds **8** and **9**) which were found to block the TRPA1 ion channel reversibly *in vitro* and alleviate TRPA1-mediated inflammation *in vivo*. They could be useful lead compounds when developing new drugs for alleviating TRPA1-mediated adverse conditions.

METHODS

Triterpenoid synthesis

General Experimental Procedures. Commercially available reagents were used without further purification. Crude betulin (UPM, Lappeenranta, Finland) was recrystallized from 2-propanol/H_2O azeotrope to yield 99% pure betulin as a white solid. All solvents were of HPLC grade. Anhydrous solvents were purchased from Sigma-Aldrich (St. Louis, MO, USA). All reactions in anhydrous solvents were performed in oven-dried glassware under an inert atmosphere of anhydrous argon or nitrogen. Thin-layer chromatography (TLC) was performed on E. Merck (Darmstadt, Germany) silica gel 60 backed plates, with visualization by UV illumination and staining with 5% H_2SO_4 in MeOH. Melting points were obtained with a Sanyo Gallenkamp (Moriguchi, Osaka, Japan) apparatus without correction. The Fourier transform infrared (FTIR) spectra were recorded on a Nicolet iS50 FT-IR (Waltham, MA, USA) using a built-in diamond ATR. The ^{1}H and ^{13}C NMR spectra were measured on a Bruker Avance III 500 MHz NMR spectrometer (Billerica, MA, USA). ^{1}H and ^{13}C NMR spectra were recorded in solution, in $CDCl_3$. HRMS were measured to determine the purity of all tested compounds on a Waters Acquity UPLC system (Waters, Milford, MA, USA) equipped with a Synapt G2 HDMS mass spectrometer (Waters).

Triterpenoids. A novel method was developed to synthesize betulonic and betulinic acid from betulin, as detailed below. The other 11 betulin derivatives were prepared as described previously [20-22].

Betulonic acid (2). Palladium(II) acetate (1.2 g, 6 w-%) and pyridine (5 mL) were added to toluene (500 mL). Mixture was heated to 80 °C and betulin (**1**) (20.0 g, 45.2 mmol) was added in small portions under vigorous stirring and air bubbling (flow rate 1000 mL/min). After 7 h, the reaction was quenched (monitored by GC) by adding *N*-acetyl-L-cysteine (8.0 g, 66.0 mmol) to scavenge Pd(II). The reaction mixture was cooled to room temperature, and the residue was filtered and washed

with toluene (3 × 20 mL). The resulting filtrate containing betulonic aldehyde was used in the next reaction step in one pot without further purification. *tert*-Butanol (170 mL) and 2-methyl-2-butene (30 mL) were added to the filtrate (containing 20 g of betulonic aldehyde, GC purity 88%) under N_2 flow. $NaClO_2$ (80%, 17.0 g, 150 mmol) and $NaH_2PO_4 \bullet H_2O$ (25.2 g, 183 mmol) in water (200 mL) were added during 30 min and stirring was continued at RT under N_2 atmosphere for 15 h. The organic and aqueous phases were separated and 1.7 M solution of NaOH in H_2O (40 mL) was added to the organic phase and stirred for 0.5 h. Half of the solvent was evaporated off *in vacuo* and the formed precipitate was filtered, washed with toluene (4 × 20 mL) and dried overnight *in vacuo* to yield sodium betulonate (16.6 g, 36.0 mmol). Sodium betulonate was treated with a 3% solution of HCl in H_2O (200 mL) and the resulting mixture was stirred for 2.5 h. The formed precipitate was filtered and washed with water (5 × 30 mL), dried *in vacuo* at 60 °C overnight to give betulonic acid (14.9 g, 32.8 mmol), in 73% yield from betulin. Spectral data was identical to that reported in the literature [21].

Betulinic acid (3). Betulonic acid (**2**) (13.0 g, 28.6 mmol) was added to a mixture of water (130 mL), 5% solution of NaOH in H_2O (26 mL) and 2-propanol (120 mL). $NaBH_4$ (1.20 g, 31.7 mmol) was added and the reaction mixture was stirred for 3 h in an ice bath. The alkaline solution was acidified by adding 10% solution of HCl in H_2O (130 mL). The precipitated betulinic acid was filtered, washed with water (4 × 50 mL) and dried *in vacuo* to yield crude betulinic acid (12.2 g, 94%). A batch of crude betulinic acid (5.0 g) was dissolved in refluxing ethanol (50 mL) and allowed to crystallize at 4 °C overnight. The formed crystals were filtrated and dried *in vacuo* to produce very pure betulinic acid (4.1 g, 9.0 mmol) in 82% yield. Spectral data was identical to that reported in the literature [21].

Effects of triterpenoids on TRPA1-mediated responses

Reagents. Reagents (unless otherwise indicated) were provided by Sigma Chemical Co., St. Louis, MO, USA.

Cell culture. HEK293 human embryonic kidney cells (American Type Culture Collection, Manassas, VA, USA) were cultured at 37 °C in 5% CO_2 in Eagle's Minimum Essential Medium (EMEM) supplemented with fetal bovine serum (10%), sodium pyruvate (1 mM), sodium bicarbonate (1.5%), non-essential amino acids (1 mM each, all from Lonza, Verviers, Belgium), streptomycin (100 mg/mL), penicillin (100 U/mL) and amphotericin B (all from Invitrogen, Paisley, UK). Cells were cultivated on a 96-well plate and transfected transiently with hTRPA1 (0.2 µg/well, pCMV6-XL4; Origene, Rockville, MD, USA) or mTRPA1 plasmid (0.2 µg/well, Mm17807; Gene Copoeia Inc., MD, USA). The cells were transfected 20 h before the experiments were started with Lipofectamine 2000 (Invitrogen, 0.5 µL/well).

Intracellular Ca^{2+} measurements. For intracellular Ca^{2+} measurements, transiently transfected HEK293 cells were loaded with Fluo 3 acetoxymethyl (AM) ester [2.5 µM Fluo 3-AM in Hanks' Basic Salt Solution (Lonza, Verviers, Belgium) pH 7.45 with 25 mM HEPES, 1 mg/mL bovine serum albumin, 2.5 mM probenecid and 0.08% Pluronic F-127®], for 40 min, at RT. Thereafter, the cells were washed and buffer solution containing the studied compounds was added to the wells and the cells were incubated for 30 min at 37 °C. Free intracellular Ca^{2+} concentrations were measured with a Victor^3 1420 multi-label counter (Perkin Elmer, Waltham, MA, USA) at wavelengths of em485/ex535 nm. Basal level of fluorescence was measured for 15 s before adding the TRPA1 agonist allyl isothiocyanate (AITC, 50 µM) and thereafter the measurements were continued for 30 s. Finally, ionomycin (1 µM), was applied to induce a robust Ca^{2+}-influx. The TRPA1-opening properties of the compounds were measured using the same protocol with the exception of adding the compounds of interest instead of AITC. In these measurements, AITC (50 µM) was used as a

positive control and the TRPA1 antagonist HC-030031 (100 – 200 μM) was utilized to estimate the TRPA1 mediation of Ca^{2+}-influx.

The cytotoxic effects of all the triterpenoids studied were evaluated with the modified XTT test (Cell Proliferation Kit II; Roche Diagnostics, Mannheim, Germany).

Whole-cell patch clamp recordings. Whole-cell patch clamp recordings were performed on HEK293 cells transiently transfected with a plasmid encoding hTRPA1 (pIRES2-AcGFP1; Takara, Tokyo, Japan). The cells successfully expressing TRPA1 were identified using green fluorescent protein. The resistance of electrodes was 3–7 MΩ when filled with a solution mimicking intracellular conditions (CsCl 30 mM, Cs aspartate 110 mM, $MgCl_2$ 1 mM, EGTA 10 mM, HEPES 10 mM, $CaCl_2$ 6.25 mM, ATP disodium salt 2 mM, adjusted to pH 7.2 with CsOH). Membrane currents and voltage signals were converted into a digital form using an analog–digital converter (PCI6229; National Instruments Japan Corporation, Tokyo, Japan). Data acquisition and current imaging of whole-cell currents were performed using WinEDR V3.38 developed by Dr. John Dempster (University of Strathclyde, UK). A ramp voltage protocol from -150 mV to +100 mV of 100 ms was applied every 5 s from a holding potential of -50 mV. A HEPES-buffered bathing solution (CsCl 10 mM, KCl 5.9 mM, NaCl 137 mM, glucose 14 mM, $MgCl_2$ 1.2 mM, HEPES 10 mM, adjusted to pH 7.4 with NaOH) was used. All experiments were performed at 25 ± 1 °C, and the studied drugs, AITC (10 and 50 μM), compound **8** (0.3 – 100 μM), compound **9** (0.3 – 100 μM), HC-030031 (30 μM), and A-967079 (5 μM) were dissolved in dimethyl sulfoxide (final concentration ≤ 0.13%).

***In vivo* model of TRPA1-mediated inflammation.** Male C57BL/6N mice were obtained from Scanbur Research A/S, Karlslunde, Denmark. The mice were housed at the Tampere University animal facility (12:12 h light:dark cycle, temperature 22 ± 1 °C, food and water provided *ad libitum*). Animal experiments were carried out in accordance with the institutional, national and European (Directive 2010/63/EU) legislation for the protection of animals used for scientific

purposes and approved by the National Animal Experiment Board. Anaesthesia was performed with ketamine (75 mg/kg, i.p., Ketalar®; Pfizer Oy Animal Health, Helsinki, Finland) and medetomidine (0.375 mg/kg, i.p., Domitor®; Orion Oyj, Espoo, Finland).

The specific TRPA1 agonist AITC was used to induce inflammatory paw edema by injecting 50 µL of sterile endotoxin-free PBS containing 15 mM AITC into the hind paw of anaesthetized mice. The contralateral paw was injected with the corresponding volume of the vehicle. Prior to the injection of AITC, the mice were dosed with either compound **8** or **9** (both 10 mg/kg in PBS/10% DMSO given intraperitoneally 1 h before AITC), or with the vehicle or with the known TRPA1 antagonist HC-030031 [300 mg/kg in 50% polyethylene glycol, 40% 1,2-propanediol and 10% Glucosteril 50 mg/mL (Baxter Oy, Vantaa, Finland) given intragastrically 2 h before AITC]. The paw volumes were measured before and 3 and 6 h after the AITC injections with a plethysmometer (Ugo Basile, Comerio, Italy). The volume change in the vehicle-injected control paw was subtracted from the volume change in the AITC-injected paw and the results are given in µL.

Statistical analysis

The statistical significance of the results was analysed with GraphPad InStat® 3.10 for Windows (GraphPad Software, Inc. San Diego, CA, USA) and with Origin9.1J (OriginLab, Northampton, MA, USA) using two-way or one-way ANOVA with Dunnett's, Bonferroni's or Tukey's multiple comparison test. The results are expressed as mean ± SEM (standard error of the mean) with *=$p<0.05$, **=$p<0.01$ and ***=$p<0.001$.

AUTHOR INFORMATION

Corresponding author

Professor Eeva Moilanen

Faculty of Medicine and Health Technology, Tampere University

33014 Tampere, Finland

Email: eeva.moilanen@tuni.fi

Author contributions

RH, TJA, AS, VAM and JY-K designed and synthetized the triterpenoids, and the chemistry part was conceived, supervised and funded by JY-K; IM-O, MH, LJM, KM and EM designed and carried out the in vitro and in vivo bioactivity experiments and data analysis, and the bioactivity part was conceived, supervised and funded by KM (patch clamp experiments) and by EM (other in vitro and in vivo experiments); IM-O drafted the manuscript and he was supported by MH, LJM, KM, JY-K and EM; all authors participated in the interpretation of the data and revised the manuscript critically for important intellectual content.

ACKNOWLEDGEMENTS

Ms Terhi Salonen is warmly thanked for skillful technical assistance, Ms Heli Määttä for superb secretarial help and Dr Ewen MacDonald for professional language editing. We acknowledge Tor, Joe and Pentti Borg Foundation, The Paulo Foundation, The Academy of Finland (project 317507) and Medical Research Fund of Tampere University Hospital for financially supporting the bioactivity studies; and European Commission (contracts. FP7-KBBE-227329-ForestSpeCs and FP7-HEALTH-602919-GLORIA), The Academy of Finland (project 252308), and Marjatta and Eino Kolli Foundation for supporting the chemistry part of this study.

REFERENCES

(1) Zygmunt, P. M. and Högestätt, E. D. (2014) Trpa1. *Handb. Exp. Pharmacol. 222,* 583-630.

(2) Koivisto, A., Chapman, H., Jalava, N., Korjamo, T., Saarnilehto, M., Lindstedt, K. and Pertovaara, A. (2014) TRPA1: a transducer and amplifier of pain and inflammation. *Basic Clin. Pharmacol. Toxicol. 114,* 50-55.

(3) Jordt, S. E., Bautista, D. M., Chuang, H. H., McKemy, D. D., Zygmunt, P. M., Högestätt, E. D., Meng, I. D. and Julius, D. (2004) Mustard oils and cannabinoids excite sensory nerve fibres through the TRP channel ANKTM1. *Nature 427,* 260-265.

(4) Bautista, D. M., Movahed, P., Hinman, A., Axelsson, H. E., Sterner, O., Hogestatt, E. D., Julius, D., Jordt, S. E. and Zygmunt, P. M. (2005) Pungent products from garlic activate the sensory ion channel TRPA1. *Proc. Natl. Acad. Sci. U. S. A. 102,* 12248-12252.

(5) Bandell, M., Story, G. M., Hwang, S. W., Viswanath, V., Eid, S. R., Petrus, M. J., Earley, T. J. and Patapoutian, A. (2004) Noxious cold ion channel TRPA1 is activated by pungent compounds and bradykinin. *Neuron 41,* 849-857.

(6) Moilanen, L. J., Laavola, M., Kukkonen, M., Korhonen, R., Leppänen, T., Högestätt, E. D., Zygmunt, P. M., Nieminen, R. M. and Moilanen, E. (2012) TRPA1 contributes to the acute inflammatory response and mediates carrageenan-induced paw edema in the mouse. *Sci. Rep. 2,* 380.

(7) Moilanen, L. J., Hämäläinen, M., Nummenmaa, E., Ilmarinen, P., Vuolteenaho, K., Nieminen, R. M., Lehtimäki, L. and Moilanen, E. (2015) Monosodium iodoacetate-induced inflammation and joint pain are reduced in TRPA1 deficient mice--potential role of TRPA1 in osteoarthritis. *Osteoarthritis Cartilage 23,* 2017-2026.

(8) Moilanen, L. J., Hämäläinen, M., Lehtimäki, L., Nieminen, R. M. and Moilanen, E. (2015) Urate crystal induced inflammation and joint pain are reduced in transient receptor potential ankyrin 1 deficient mice--potential role for transient receptor potential ankyrin 1 in gout. *PLoS One 10,* e0117770.

(9) Trevisan, G., Hoffmeister, C., Rossato, M. F., Oliveira, S. M., Silva, M. A., Ineu, R. P., Guerra, G. P., Materazzi, S., Fusi, C., Nassini, R., Geppetti, P. and Ferreira, J. (2013) Transient Receptor Potential Ankyrin 1 Receptor Stimulation by Hydrogen Peroxide Is Critical to Trigger Pain During Monosodium Urate–Induced Inflammation in Rodents. *Arthritis & Rheumatism 65,* 2984-2995.

(10) McNamara, C. R., Mandel-Brehm, J., Bautista, D. M., Siemens, J., Deranian, K. L., Zhao, M., Hayward, N. J., Chong, J. A., Julius, D., Moran, M. M. and Fanger, C. M. (2007) TRPA1 mediates formalin-induced pain. *Proc. Natl. Acad. Sci. U. S. A. 104,* 13525-13530.

(11) Takahashi, N., Mizuno, Y., Kozai, D., Yamamoto, S., Kiyonaka, S., Shibata, T., Uchida, K. and Mori, Y. (2008) Molecular characterization of TRPA1 channel activation by cysteine-reactive inflammatory mediators. *Channels (Austin) 2,* 287-298.

(12) Xu, R., Fazio, G. C. and Matsuda, S. P. T. (2004) On the origins of triterpenoid skeletal diversity. *Phytochemistry 65,* 261-291.

(13) Jäger, S., Trojan, H., Kopp, T., Laszczyk, M. N. and Scheffler, A. (2009) Pentacyclic triterpene distribution in various plants - rich sources for a new group of multi-potent plant extracts. *Molecules 14,* 2016-2031.

(14) He, X. and Liu, R. H. (2007) Triterpenoids isolated from apple peels have potent antiproliferative activity and may be partially responsible for apple's anticancer activity. *J. Agric. Food Chem. 55,* 4366-4370.

(15) Laavola, M., Haavikko, R., Hämäläinen, M., Leppänen, T., Nieminen, R., Alakurtti, S., Moreira, V. M., Yli-Kauhaluoma, J. and Moilanen, E. (2016) Betulin Derivatives Effectively Suppress Inflammation in Vitro and in Vivo. *J. Nat. Prod. 79,* 274-280.

(16) Dehelean, C. A., Soica, C., Ledeti, I., Aluas, M., Zupko, I., G Luscan, A., Cinta-Pinzaru, S. and Munteanu, M. (2012) Study of the betulin enriched birch bark extracts effects on human carcinoma cells and ear inflammation. *Chem. Cent. J. 6,* 137-153X-6-137.

(17) Sun, I. C., Shen, J. K., Wang, H. K., Cosentino, L. M. and Lee, K. H. (1998) Anti-AIDS agents. 32. Synthesis and anti-HIV activity of betulin derivatives. *Bioorg. Med. Chem. Lett. 8,* 1267-1272.

(18) Duker-Eshun, G., Jaroszewski, J. W., Asomaning, W. A., Oppong-Boachie, F. and Brogger Christensen, S. (2004) Antiplasmodial constituents of Cajanus cajan. *Phytother. Res. 18,* 128-130.

(19) Alakurtti, S., Bergstrom, P., Sacerdoti-Sierra, N., Jaffe, C. L. and Yli-Kauhaluoma, J. (2010) Anti-leishmanial activity of betulin derivatives. *J. Antibiot. (Tokyo) 63,* 123-126.

(20) Alakurtti, S., Heiska, T., Kiriazis, A., Sacerdoti-Sierra, N., Jaffe, C. L. and Yli-Kauhaluoma, J. (2010) Synthesis and anti-leishmanial activity of heterocyclic betulin derivatives. *Bioorg. Med. Chem. 18,* 1573-1582.

(21) Pohjala, L., Alakurtti, S., Ahola, T., Yli-Kauhaluoma, J. and Tammela, P. (2009) Betulin-derived compounds as inhibitors of alphavirus replication. *J. Nat. Prod. 72,* 1917-1926.

(22) Haavikko, R., Nasereddin, A., Sacerdoti-Sierra, N., Kopelyanskiy, D., Alakurtti, S., Tikka, M., Jaffe, C. L. and Yli-Kauhaluoma, J. (2014) Heterocycle-fused lupane triterpenoids inhibit Leishmania donovani amastigotes. *Med. Chem. Commun. 5,* 445-451.

(23) Fulda, S. and Debatin, K. M. (2005) Sensitization for anticancer drug-induced apoptosis by betulinic Acid. *Neoplasia 7,* 162-170.

(24) Ehrhardt, H., Fulda, S., Fuhrer, M., Debatin, K. M. and Jeremias, I. (2004) Betulinic acid-induced apoptosis in leukemia cells. *Leukemia 18,* 1406-1412.

(25) Kim, S., Ryu, H. G., Lee, J., Shin, J., Harikishore, A., Jung, H., Jung, H., Kim, Y. S., Lyu, H., Oh, E., Baek, N., Choi, K., Yoon, H. S. and Kim, K. (2015) Ursolic acid exerts anti-cancer

activity by suppressing vaccinia-related kinase 1-mediated damage repair in lung cancer cells. *Scientific Reports 5*, 14570.

(26) Klement, G., Eisele, L., Malinowsky, D., Nolting, A., Svensson, M., Terp, G., Weigelt, D. and Dabrowski, M. (2013) Characterization of a ligand binding site in the human transient receptor potential ankyrin 1 pore. *Biophys. J. 104*, 798-806.

(27) Gupta, R., Saito, S., Mori, Y., Itoh, S. G., Okumura, H. and Tominaga, M. (2016) Structural basis of TRPA1 inhibition by HC-030031 utilizing species-specific differences. *Scientific Reports 6*, 37460.

(28) Xiao, B., Dubin, A. E., Bursulaya, B., Viswanath, V., Jegla, T. J. and Patapoutian, A. (2008) Identification of transmembrane domain 5 as a critical molecular determinant of menthol sensitivity in mammalian TRPA1 channels. *J. Neurosci. 28*, 9640-9651.

(29) Moilanen, L. J., Hämäläinen, M., Lehtimäki, L., Nieminen, R. M., Muraki, K. and Moilanen, E. (2016) Pinosylvin Inhibits TRPA1-Induced Calcium Influx In Vitro and TRPA1-Mediated Acute Paw Inflammation In Vivo. *Basic Clin. Pharmacol. Toxicol. 118*, 238-242.

(30) Trevisan, G., Rossato, M. F., Tonello, R., Hoffmeister, C., Klafke, J. Z., Rosa, F., Pinheiro, K. V., Pinheiro, F. V., Boligon, A. A., Athayde, M. L. and Ferreira, J. (2014) Gallic acid functions as a TRPA1 antagonist with relevant antinociceptive and antiedematogenic effects in mice. *Naunyn Schmiedebergs Arch. Pharmacol. 387*, 679-689.

(31) Schenkel, L. B., Olivieri, P. R., Boezio, A. A., Deak, H. L., Emkey, R., Graceffa, R. F., Gunaydin, H., Guzman-Perez, A., Lee, J. H., Teffera, Y., Wang, W., Youngblood, B. D., Yu, V. L., Zhang, M., Gavva, N. R., Lehto, S. G. and Geuns-Meyer, S. (2016) Optimization of a Novel Quinazolinone-Based Series of Transient Receptor Potential A1 (TRPA1) Antagonists Demonstrating Potent in Vivo Activity. *J. Med. Chem. 59*, 2794-2809.

(32) Chen, H., Volgraf, M., Do, S., Kolesnikov, A., Shore, D. G., Verma, V. A., Villemure, E., Wang, L., Chen, Y., Hu, B., Lu, A., Wu, G., Xu, X., Yuen, P., Zhang, Y., Erickson, S. D., Dahl, M., Brotherton-Pleiss, C., Tay, S., Ly, J. Q., Murray, L. J., Chen, J., Amm, D., Lange, W., Hackos, D. H., Reese, R. M., Shields, S. D., Lyssikatos, J. P., Safina, B. S. and Estrada, A. A. (2018) Discovery of a Potent (4R,5S)-4-Fluoro-5-methylproline Sulfonamide Transient Receptor Potential Ankyrin 1 Antagonist and Its Methylene Phosphate Prodrug Guided by Molecular Modeling. *J. Med. Chem. 61*, 3641-3659.

(33) Nummenmaa, E., Hämäläinen, M., Moilanen, L. J., Paukkeri, E. L., Nieminen, R. M., Moilanen, T., Vuolteenaho, K. and Moilanen, E. (2016) Transient receptor potential ankyrin 1 (TRPA1) is functionally expressed in primary human osteoarthritic chondrocytes. *Arthritis Res. Ther. 18*, 185-016-1080-4.

(34) Gijsen, H. J., Berthelot, D., De Cleyn, M. A., Geuens, I., Brone, B. and Mercken, M. (2012) Tricyclic 3,4-dihydropyrimidine-2-thione derivatives as potent TRPA1 antagonists. *Bioorg. Med. Chem. Lett. 22*, 797-800.

(35) Atoyan, R., Shander, D. and Botchkareva, N. V. (2009) Non-Neuronal Expression of Transient Receptor Potential Type A1 (TRPA1) in Human Skin. *J. Invest. Dermatol. 129*, 2312-2315.

(36) Glenmark's TRPA1 antagonist 'GRC 17536' shows positive data in a proof of concept study. *http://www.prnewswire.com* (accessed 2016/10/4, 2014).

(37) Liu, B., Escalera, J., Balakrishna, S., Fan, L., Caceres, A. I., Robinson, E., Sui, A., McKay, M. C., McAlexander, M. A., Herrick, C. A. and Jordt, S. E. (2013) TRPA1 controls inflammation and pruritogen responses in allergic contact dermatitis. *FASEB Journal 27*, 3549-3563.

(38) Caceres, A. I., Brackmann, M., Elia, M. D., Bessac, B. F., del Camino, D., D'Amours, M., Witek, J. S., Fanger, C. M., Chong, J. A., Hayward, N. J., Homer, R. J., Cohn, L., Huang, X., Moran, M. M. and Jordt, S. E. (2009) A sensory neuronal ion channel essential for airway inflammation and hyperreactivity in asthma. *Proc. Natl. Acad. Sci. U. S. A. 106*, 9099-9104.

(39) Engel, M. A., Leffler, A., Niedermirtl, F., Babes, A., Zimmermann, K., Filipović, M. R., Izydorczyk, I., Eberhardt, M., Kichko, T. I., Mueller-Tribbensee, S. M., Khalil, M., Siklosi, N., Nau, C., Ivanović-Burmazović, I., Neuhuber, W. L., Becker, C., Neurath, M. F. and Reeh, P. W. (2011) TRPA1 and substance P mediate colitis in mice. *Gastroenterology 141*, 1346-1358.

(40) Chen, J. and Hackos, D. H. (2015) TRPA1 as a drug target--promise and challenges. *Naunyn Schmiedebergs Arch. Pharmacol. 388*, 451-463.

Table legends

Table 1

The effect of triterpenoids (10 µM) on allyl isothiocyanate (AITC, 50 µM)-induced TRPA1 activation measured by Ca^{2+} influx in HEK293 cells transfected with a plasmid encoding hTRPA1. TRPA1-inhibition by triterpenoids is presented as a percentage of the area under curve (AUC) in relation to the untreated AITC control. Results are expressed as mean ± SEM, *$p < 0.05$, **$p < 0.01$ and ***$p < 0.001$.

Figure legends

Figure 1

Structural formulae of betulin and its triterpenoid derivatives.

Figure 2

Synthesis of betulonic (2) and betulinic (3) acid from betulin (1). Reagents and conditions: (a) $Pd(OAc)_2$, py, toluene, air, 80 °C, 7 h; (b) $NaClO_2$, $NaH_2PO_4 \bullet H_2O$, 2-methyl-2-butene, *tert*-butanol, H_2O, rt, 12 h; (c) $NaBH_4$, NaOH, H_2O, 2-propanol, 0 °C, 3 h.

Figure 3

Structural formulae of the key triterpenoids 8 and 9.

Figure 4

Compounds 8 and 9 inhibited allyl isothiocyanate (AITC, 50 µM)-induced Ca^{2+}-influx in HEK293 cells transfected with a plasmid encoding hTRPA1 in a dose-dependent manner. Fluo 3-AM loaded cells were pre-incubated for 30 min with compound **8** (1 – 100 µM), compound **9** (1 – 100 µM) or with the known TRPA1 antagonist HC-030031 (100/200 µM) before intracellular Ca^{2+} measurement. **A** and **C** show representative curves displaying relative fluorescence units after treatment with compounds **8** and **9**, respectively. **B** and **D** show the areas under curve (AUC; from 15 to 45s) of the response to AITC with or without compound **8** and **9** treatments, respectively. Background fluorescence was recorded for 15 s before the addition of the TRPA1 agonist AITC. Fluorescence increase in response to AITC was measured for 30 s after which the control ionophore, ionomycin (1 µM), was added and fluorescence was measured for another 30 s. The results are normalized to the background and expressed as mean + SEM, n = 6 – 8, *$p < 0.05$, **$p < 0.01$ and ***$p < 0.001$.

Figure 5

Triterpenoids 8 and 9 inhibited allyl isothiocyanate (AITC, 50 μM) induced Ca^{2+} influx in HEK293 cells transfected with a plasmid encoding mTRPA1. Fluo 3-AM loaded cells were pre-incubated for 30 min with compound **8** (100 μM), compound **9** (100 μM) or with the known TRPA1 antagonist HC003031 (100 μM). In **A** and **B,** the areas under curve (AUC) of the fluorescence response to AITC with or without **8** and **9** treatment, respectively, are presented. Background fluorescence was recorded for 15 s before addition of AITC. The increase in fluorescence in response to AITC was measured for 30 s. The results are normalized to background and expressed as mean + SEM, n = 5-8, *p < 0.05, **p < 0.01, ***p < 0.001.

Figure 6

Triterpenoids 8 and 9 inhibited allyl isothiocyanated (AITC) -induced membrane currents measured with whole-cell patch clamp recording in HEK293 cells transfected with hTRPA1. In **A** and **C**, the current trace displays the change of inward currents at -50 mV which was evoked by compounds **8** (0.3, 3, and 30 μM) and **9** (0.3, 3, and 30 μM), respectively, in the presence of 50 μM AITC. To determine the zero current level of TRPA1 components, 30 μM HC-030031 (HC) was applied at the end of each experiment. In **B** and **D**, a current-voltage (I-V) relationship was constructed to use a ramp waveform pulse from -150 to +100 mV for 100 ms. Six I-V relationships were illustrated before (cont) and after application of AITC (50 μM AITC), and during simultaneous application of 0.3, 3, or 30 μM compound **8** (+30 μM **8**) and 50 μM AITC in **B**. The experimental conditions in **D** were identical to those utilized in **B** except for application of compound **9**. In **E** and **F**, each relative amplitude (relative) was calculated as a current size at -100, -50, +50, and +100 mV between before and after application of **8** and **9**, respectively, and

summarized as a dose-response relationship. Maximum and minimum amplitudes of the current were obtained in the presence of AITC (1.0) and in the presence of both AITC and HC-030031 (0). The results in **E** and **F** are expressed as mean ± SEM. * = $p < 0.05$ by two-way ANOVA. In **E** and **F**, the numbers of replicates are described in parentheses next to the markers.

Figure 7

Recovery of allyl isothiocyanate (AITC) -induced membrane currents after removal of compounds 8 and 9. In **A** and **D**, the trace displays the change of inward currents at -50 mV which was evoked by application and removal of compounds **8** (0.3 μM) and **9** (0.3 μM), respectively, in the presence of 10 μM AITC. To determine the zero-current level of TRPA1 components, the known TRPA1 antagonist A-967079 (A96, 5 μM) was applied at the end of each experiment. The experimental conditions in **B** and **E** and in **C** and **D** were identical to those utilized in **A** and **D** except for the concentration of compounds **8** and **9** at 3 μM and 30 μM, respectively. In **G** and **H**, the relative amplitude was calculated as a current size at -50 mV between the zero current and the current amplitude before and after application of each compound, and after their removal but still in the presence of AITC. The results in **G** and **H** are expressed as mean ± SEM, * = $p < 0.05$ against each first column and # = $p < 0.05$ against each second column, tested by Tukey's multiple comparison test. In **G** and **H**, the numbers of replicates are described in parentheses above the columns.

Figure 8

Triterpenoids 8 and 9 inhibited TRPA1-mediated acute paw inflammation in mice. Mice were pre-treated with compound **8** (10 mg/kg, i.p.), compound **9** (10 mg/kg, i.p.), the known TRPA1 blocker HC-030031 (300 mg/kg, i.g.) or with the vehicle at 1 h (**8**, **9** and vehicle) or 2 h (HC-

030031) prior to the subcutaneous administration of the TRPA1 agonist allyl isothiocyanate (AITC) in the paw. The paw volume was measured with a plethysmometer before and 3 and 6 h after AITC paw injection. The results are normalized to the control paw injected with the vehicle. Mean + SEM, n = 6, *p < 0.05, **p < 0.01, ***p < 0.001

Tables

Table 1

Compound	**% of control**
control	100
HC-030031 (100 µM)	22.24 ±2.2 ***
1 (10 µM)	98.89 ±4.0
2 (10 µM)	83.32 ±8.9
3 (10 µM)	83.65 ±3.9
4 (10 µM)	83.42 ±5.0
5 (10 µM)	85.52 ±3.2 *
6 (10 µM)	79.08 ±3.2 **
7 (10 µM)	79.55 ±4.2 **
8 (10 µM)	61.32 ±3.1 **
9 (10 µM)	64.09 ±4.0 **
10 (10 µM)	85.65 ±15.1
11 (10 µM)	86.48 ±6.6
12 (10 µM)	96.48 ±6.3
13 (10 µM)	96.90 ±6.8
14 (10 µM)	75.50 ±6.0 **

Figures

Figure 1

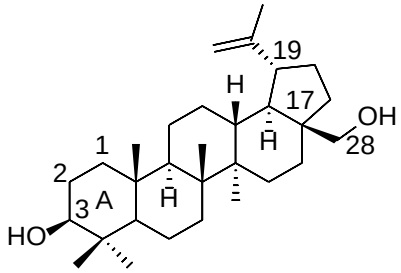

Betulin (1)

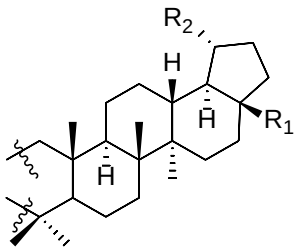

General structure (2-11)

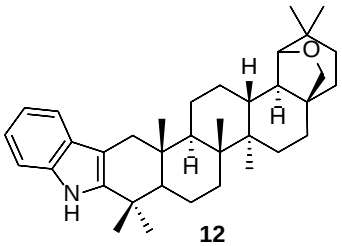

12

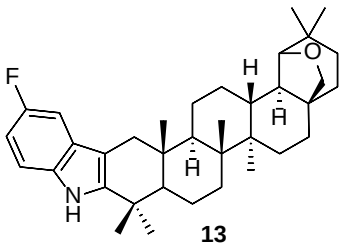

13

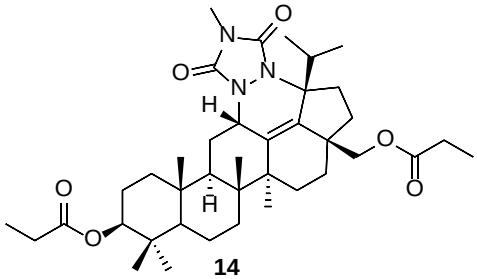

14

Author's Note: the figure continues on the next page

Figure 1 continues

Compound	Ring A	R_1	R_2
2	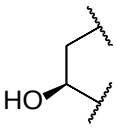	COOH	$C(=CH_2)CH_3$
3	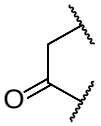	COOH	$C(=CH_2)CH_3$
4	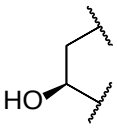	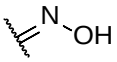	$C(=CH_2)CH_3$
5	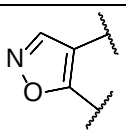	COOH	$CH(CH_3)_2$
6	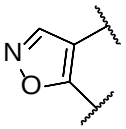		$C(=CH_2)CH_3$
7	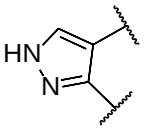	COOH	$C(=CH_2)CH_3$
8	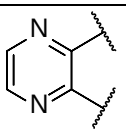	COOH	$C(=CH_2)CH_3$
9	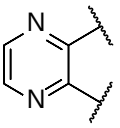	$CONH_2$	$C(=CH_2)CH_3$
10	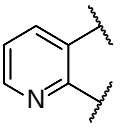	COOH	$C(=CH_2)CH_3$
11	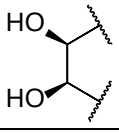	COOH	$C(=CH_2)CH_3$

Figure 2

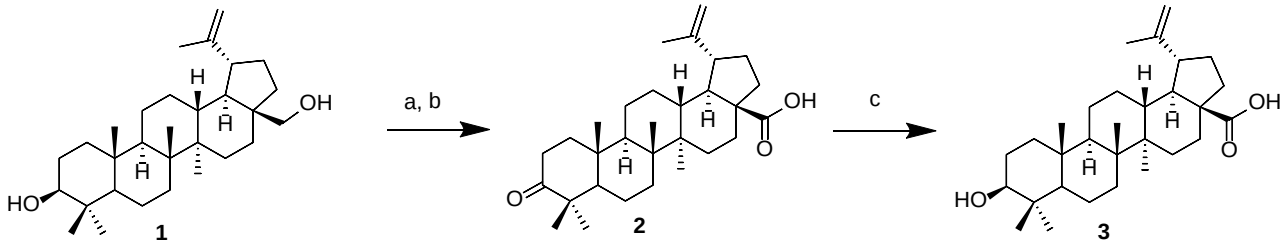

Figure 3

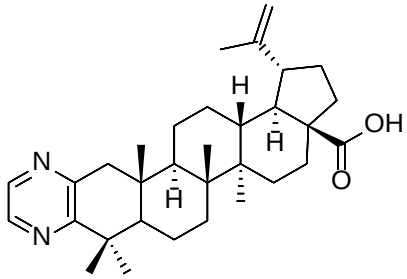

8

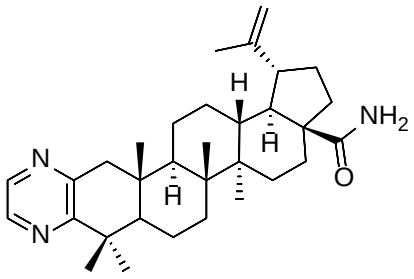

9

Figure 4 A

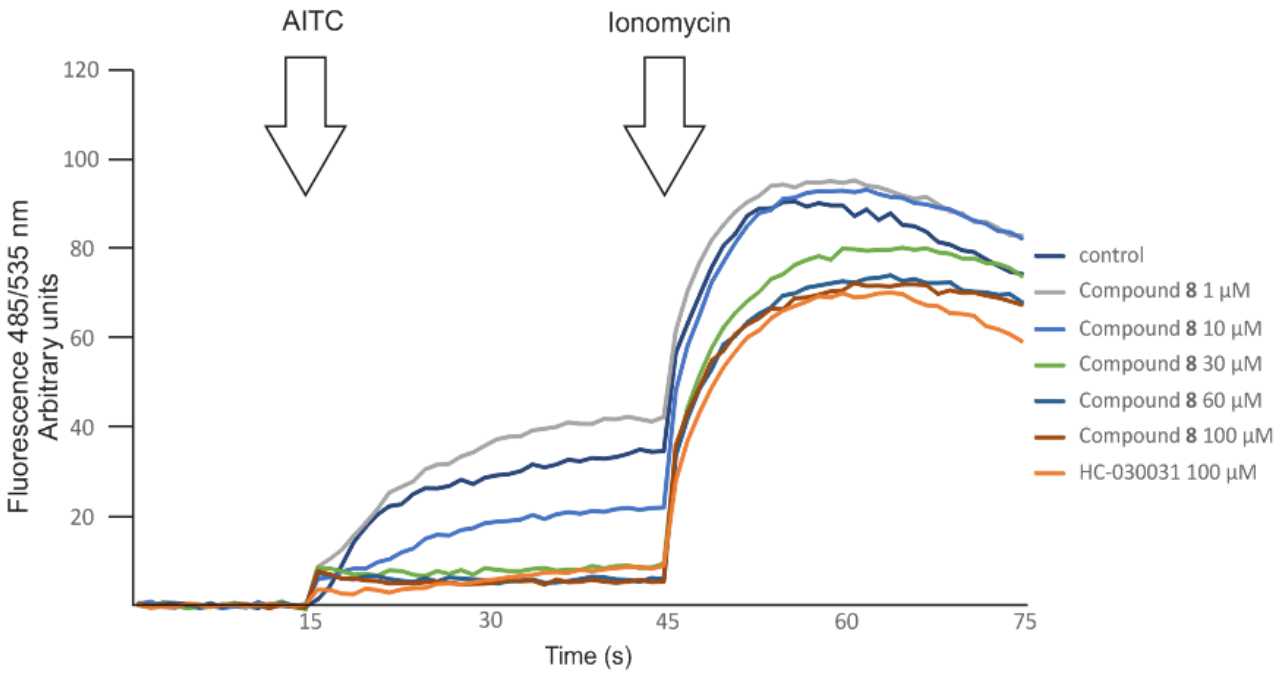

Figure 4 B

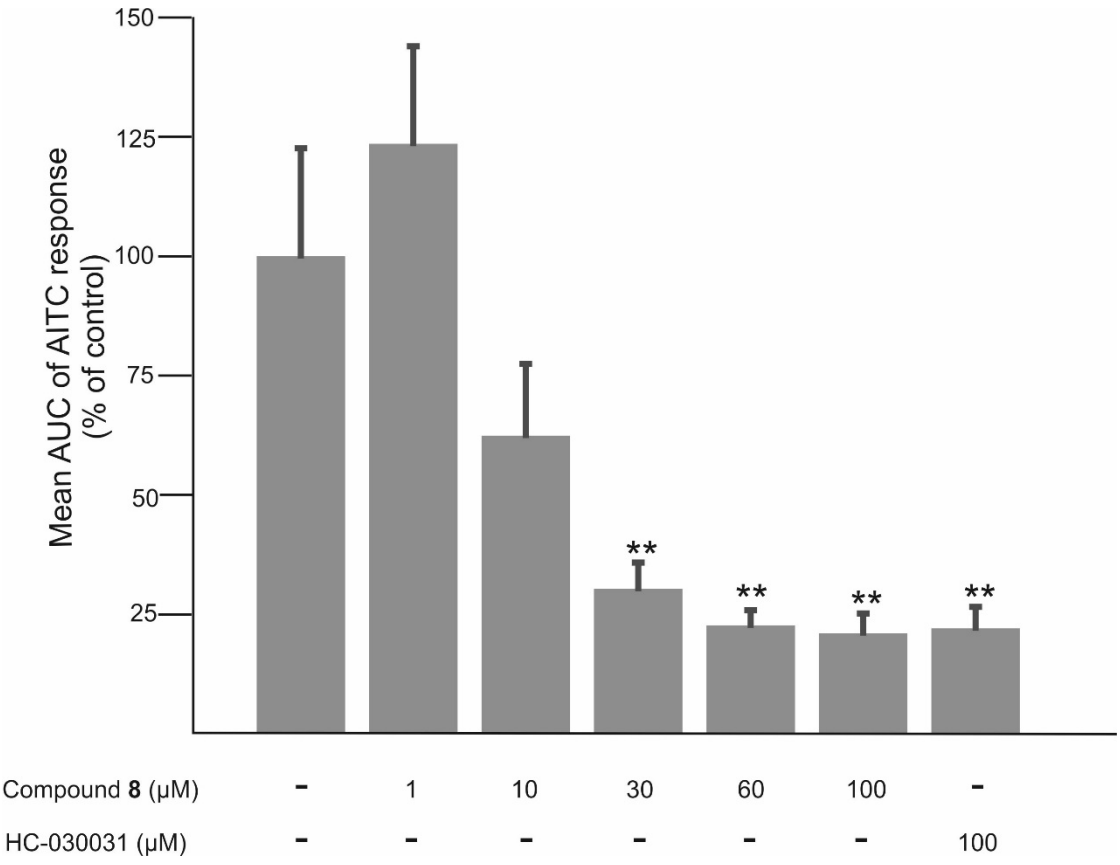

Figure 4 C

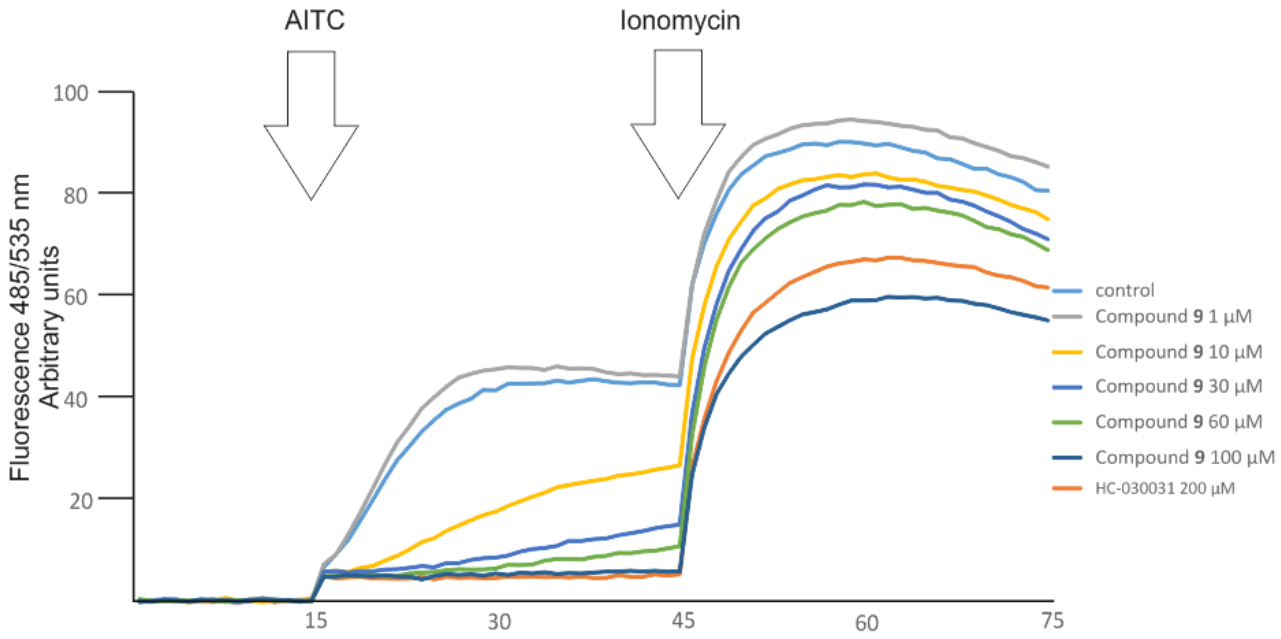

Figure 4 D

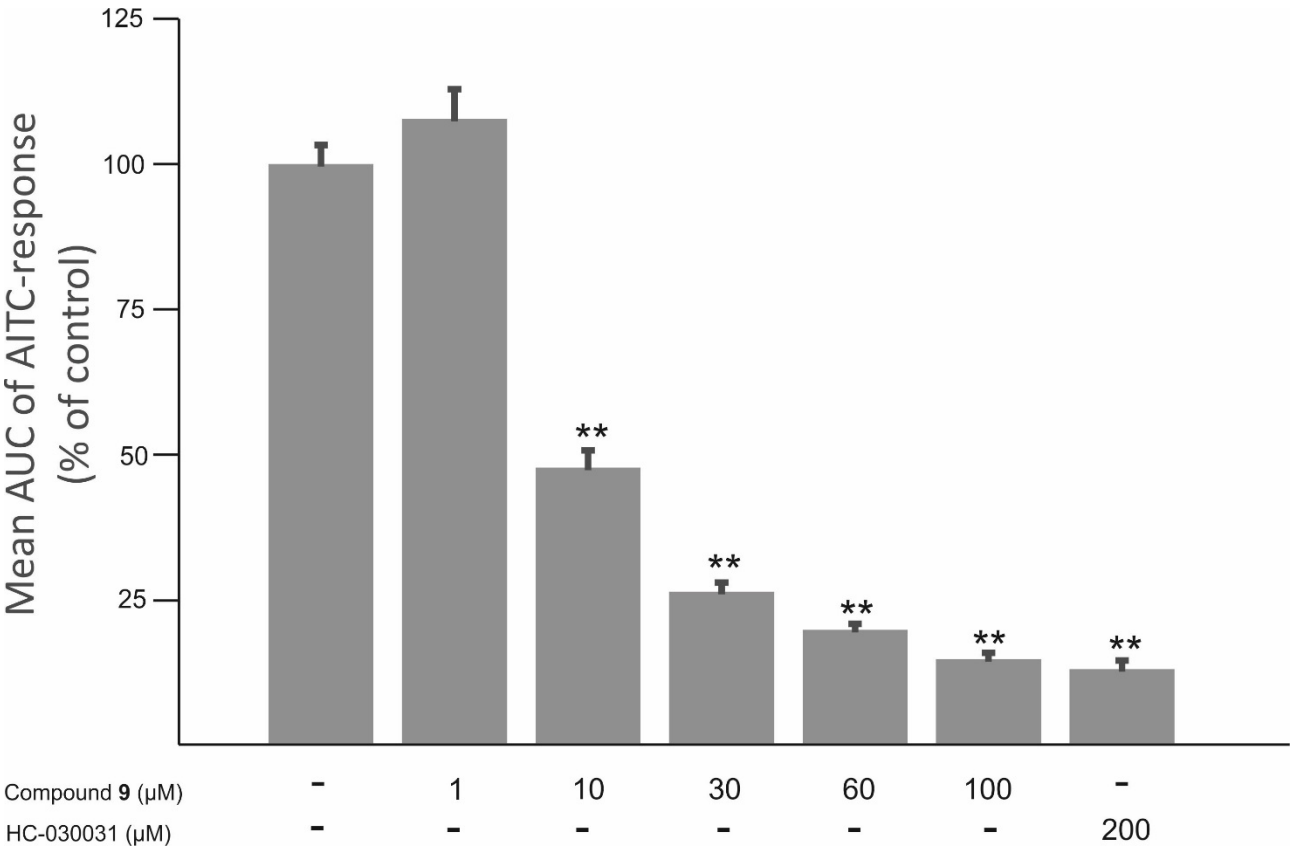

Figure 5 A

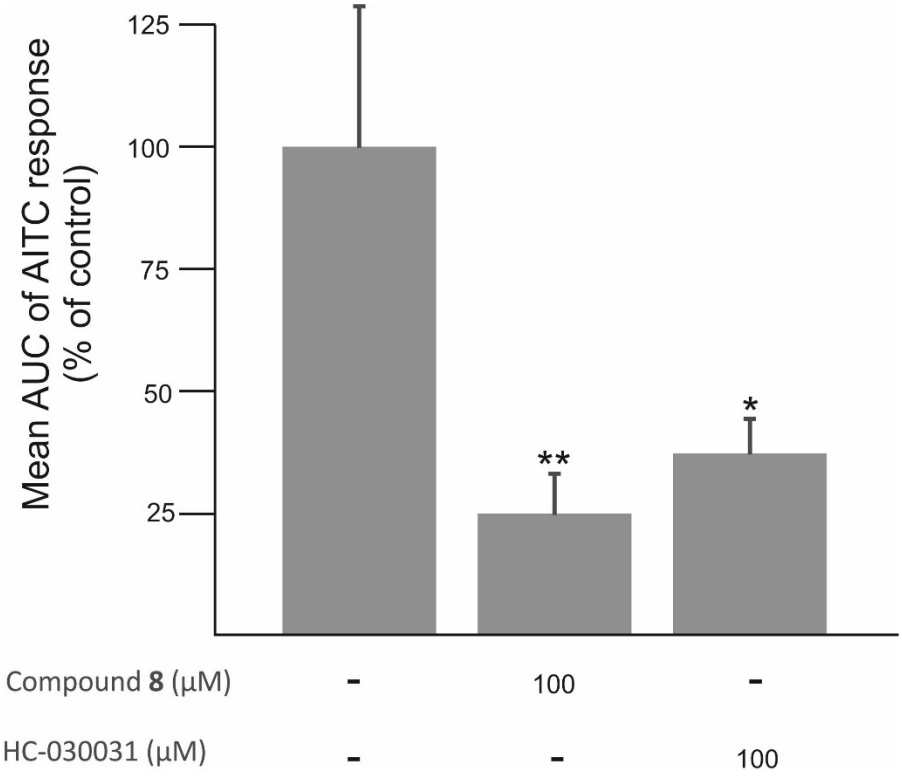

Figure 5 B

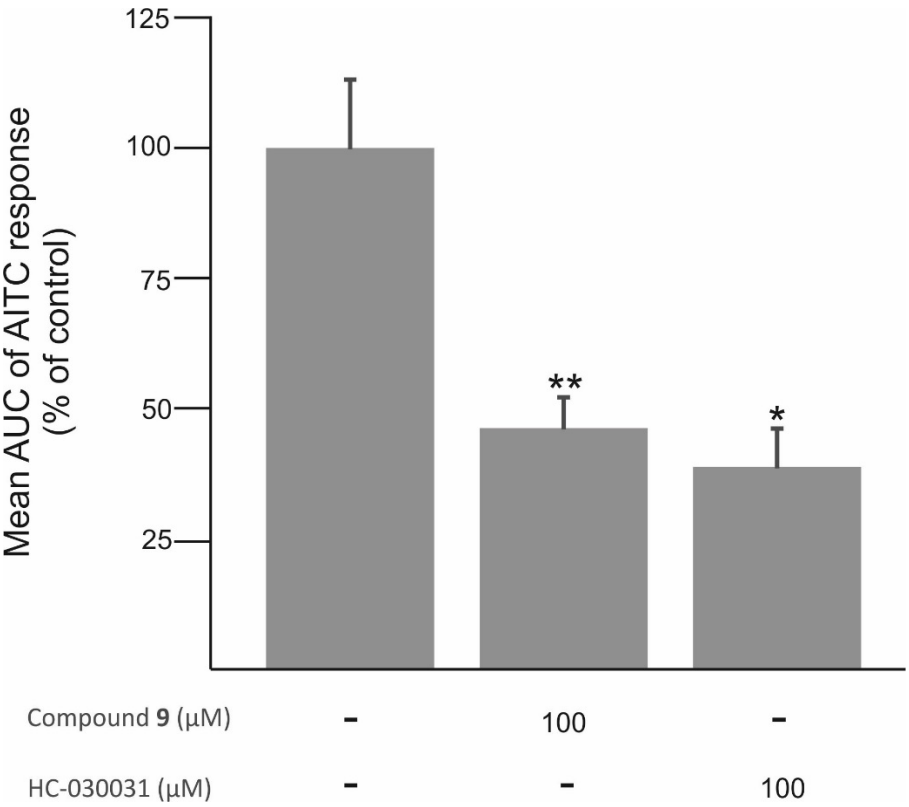

Figure 6

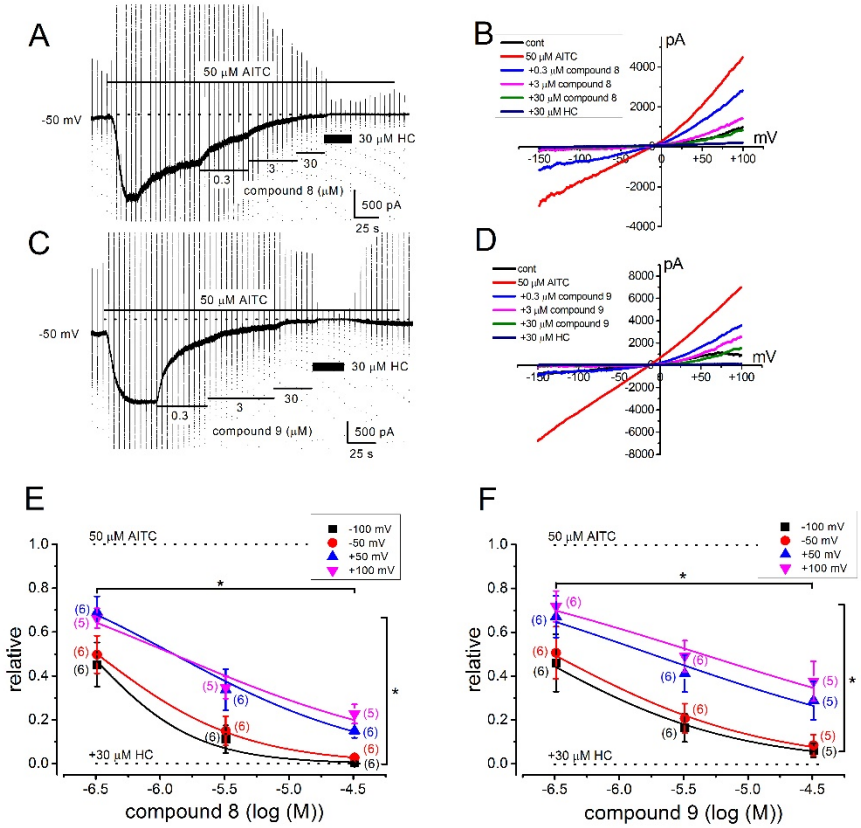
A
50 μM AITC
-50 mV
30 μM HC
0.3
3
30
compound 8 (μM)
500 pA
25 s
B
cont
50 μM AITC
+0.3 μM compound 8
+3 μM compound 8
+30 μM compound 8
+30 μM HC
pA
mV
C
50 μM AITC
-50 mV
30 μM HC
0.3
3
30
compound 9 (μM)
500 pA
25 s
D
cont
50 μM AITC
+0.3 μM compound 9
+3 μM compound 9
+30 μM compound 9
+30 μM HC
pA
mV
E
50 μM AITC
-100 mV
-50 mV
+50 mV
+100 mV
+30 μM HC
relative
compound 8 (log (M))
F
50 μM AITC
-100 mV
-50 mV
+50 mV
+100 mV
+30 μM HC
relative
compound 9 (log (M))

Figure 7

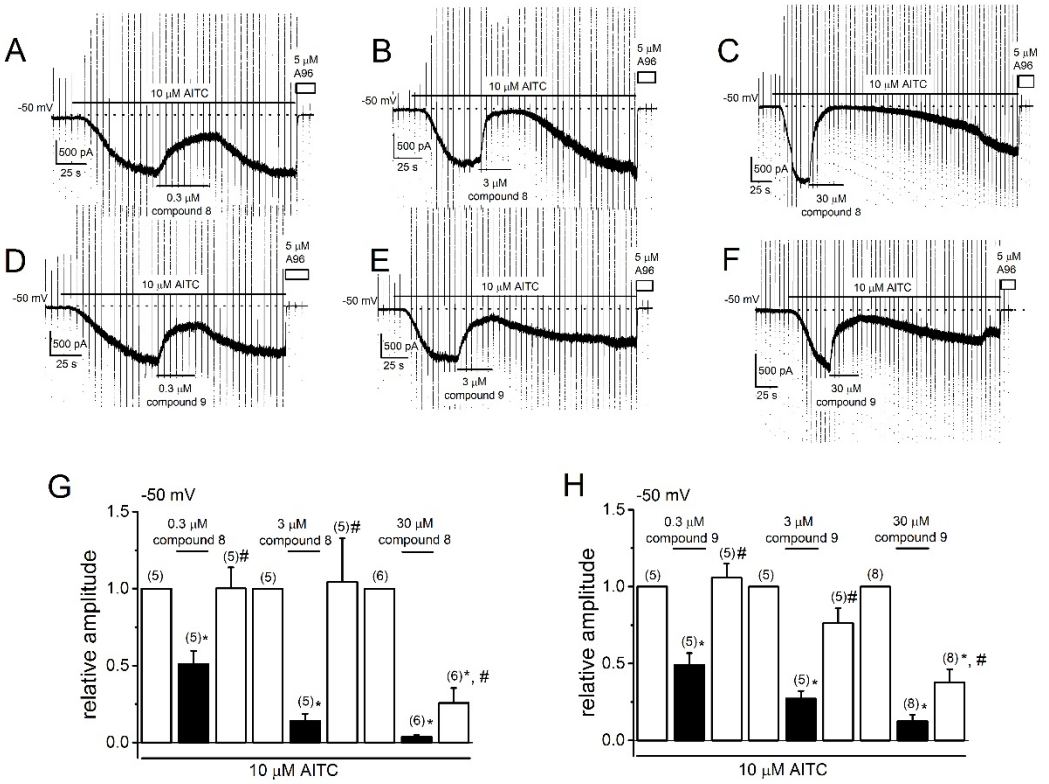
A
B
C
D
E
F
-50 mV
10 μM AITC
5 μM A96
500 pA
25 s
0.3 μM compound 8
3 μM compound 8
30 μM compound 8
0.3 μM compound 9
3 μM compound 9
30 μM compound 9

G
H
-50 mV
relative amplitude
1.5
1.0
0.5
0.0
0.3 μM compound 8
3 μM compound 8
30 μM compound 8
0.3 μM compound 9
3 μM compound 9
30 μM compound 9
(5)
(5)*
(5)#
(6)*, #
(8)
(8)*
(8)*, #
10 μM AITC

Figure 8

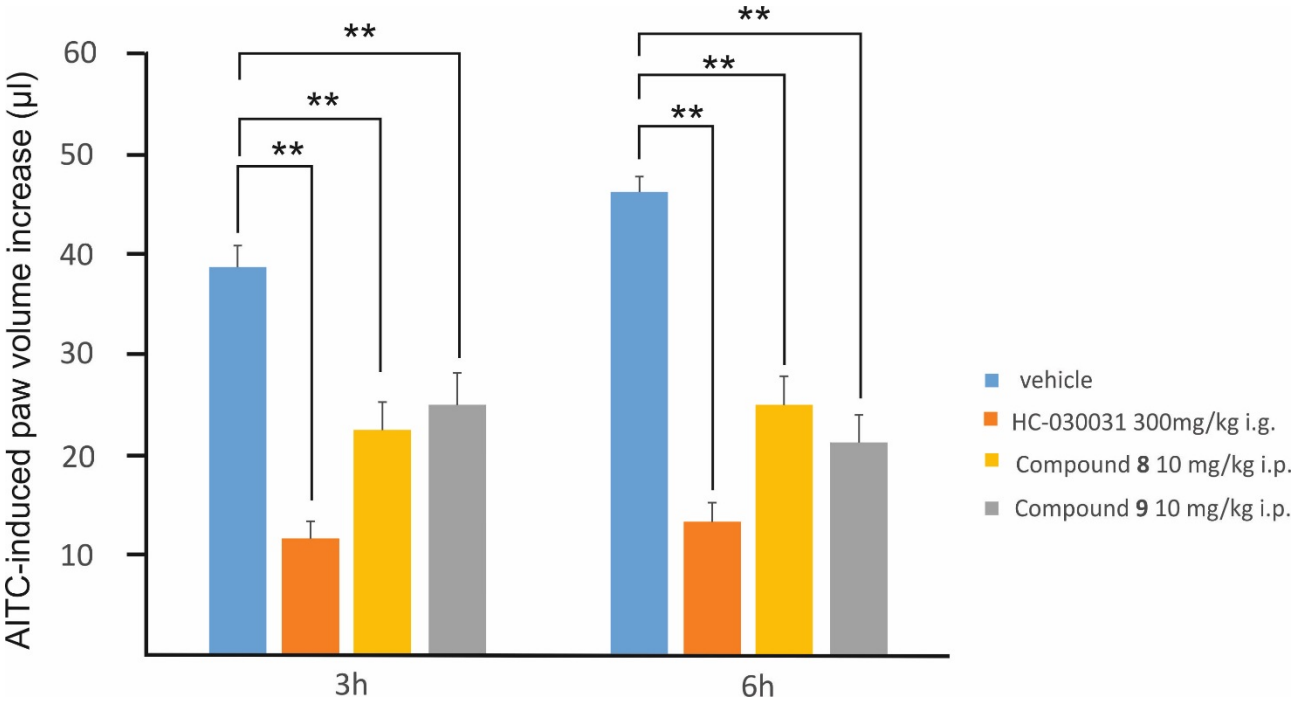
AITC-induced paw volume increase (µl)
60
50
40
30
20
10
**
**
**
**
**
**
3h
6h
vehicle
HC-030031 300mg/kg i.g.
Compound 8 10 mg/kg i.p.
Compound 9 10 mg/kg i.p.